MODELING ALL-ATOM GLYCAN STRUCTURES VIA HIERARCHICAL MESSAGE PASSING AND MULTI-SCALE PRE-TRAINING

Anonymous authors
Paper under double-blind review

ABSTRACT

Understanding the various properties of glycans with machine learning has shown some preliminary promise. However, previous methods mainly focused on modeling the backbone structure of glycans as graphs of monosaccharides (*i.e.*, sugar units), while they neglected the atomic structures underlying each monosaccharide, which are actually important indicators of glycan properties. In this work, we fill this blank by introducing the **GlycanAA** model for **A**ll-**A**tom-wise **Glycan** modeling. GlycanAA models a glycan as a heterogeneous graph with monosaccharide nodes representing its global backbone structure and atom nodes representing its local atomic-level structures. Based on such a graph, GlycanAA performs *hierarchical message passing* to capture from local atomic-level interactions to global monosaccharide-level interactions hierarchically. To further enhance the model capability, we pre-train GlycanAA on a high-quality unlabeled glycan dataset in a self-supervised way, deriving the **PreGlycanAA** model. Specifically, we design a *multi-scale mask prediction* algorithm to endow the model with knowledge about different levels of dependencies in a glycan. Extensive benchmark results show the superiority of GlycanAA over existing glycan encoders and verify the further improvements achieved by PreGlycanAA.

1 INTRODUCTION

Glycans, complex macromolecules composed of sugar molecules, play pivotal roles in life science. They serve as essential structural components in cells, forming the backbone of extracellular matrices and cell membranes (Yanagishita, 1993). Based on such structures, they modulate intercellular communication (Liu & Wang, 2023) and impact biological processes such as immune response (Zhang, 2006) and cell differentiation (Lau et al., 2007). With the accumulation of glycan data in public repositories (Tiemeyer et al., 2017; Yamada et al., 2020), it is a promising way to understand various glycan properties and functions with data-driven methods like machine learning.

In this research direction, most existing works (Burkholz et al., 2021; Lundstrøm et al., 2022; Carpenter et al., 2022; Alkuhlani et al., 2023) model a glycan as a graph with monosaccharides (*i.e.*, sugar units) as its nodes, and use graph neural networks (GNNs) to predict various glycan properties, *e.g.*, glycosylation, immunogenicity, binding affinity with a protein, *etc.* Though performing well on some tasks, these methods fail to capture the atomic-level structures underlying each monosaccharide, which are actually important determinants of many glycan properties and functions. For example, atomic-level interactions between a glycan and a protein determine their binding affinity.

There have been some preliminary attempts at modeling all-atom-wise glycan structures with state-of-the-art small molecule encoders Xu et al. (2024). However, because of the gap between a small molecule with tens of atoms and a glycan with hundreds of atoms (*i.e.*, essentially a macromolecule), these small molecule encoders are shown to be ineffective, which perform even worse than the models utilizing only monosaccharide-level information. Therefore, it is still to be answered how to realize the potential of all-atom glycan modeling on boosting glycan understanding.

To answer this question, in this work, we propose the **GlycanAA** model for **A**ll-**A**tom-wise **Glycan** modeling. Note that, a glycan naturally possesses a hierarchical structure with (1) atoms making up the local structure of each monosaccharide and (2) different monosaccharides making up the global

backbone structure of the glycan. Inspired by this fact, we design GlycanAA based on a hierarchical modeling approach. Specifically, GlycanAA first represents a glycan as a heterogeneous graph consisting of (1) a set of atom nodes for its local structures and (2) a set of monosaccharide nodes for its global structure. Based on such a graph, GlycanAA then performs *hierarchical message passing* to model from local atomic-level interactions to global monosaccharide-level interactions. In this way, GlycanAA can completely capture the covalent bonds forming each monosaccharide and the glycosidic bonds forming the whole glycan.

To further enhance the representation power of GlycanAA, we seek to endow it with the knowledge stored in abundant unlabeled glycan data. We resort to self-supervised pre-training to achieve this goal, where the **PreGlycanAA** model is developed as a pre-trained version of GlycanAA. Specifically, we first curate an unlabeled glycan dataset by selecting 40,781 high-quality glycan data from the GlyTouCan database (Tiemeyer et al., 2017). GlycanAA is then pre-trained on this dataset with a *multi-scale mask prediction* algorithm. In this algorithm, partial atom and monosaccharide nodes are masked at the input, and the model is asked to recover these masked nodes. Through this approach, the derived PreGlycanAA model acquires the dependencies between different atoms and monosaccharides in a glycan, leading to informative glycan representations.

We evaluate the proposed models on the GlycanML benchmark (Xu et al., 2024). Experimental results show that PreGlycanAA and GlycanAA respectively rank first and second on the benchmark, and they substantially outperform SOTA atomic-level small molecule encoders and glycan-specific monosaccharide-level encoders. We further demonstrate the effectiveness of the proposed hierarchical message passing and multi-scale mask prediction methods through extensive ablation studies.

2 Related Work

Glycan modeling with machine learning. With the growing size of experimental glycomics datasets, machine learning techniques are becoming increasingly important in glycoinformatics (Bojar & Lisacek, 2022; Li et al., 2022). Traditional machine learning approaches, such as support vector machines (SVMs), have been employed to learn patterns from mass spectrometry data (Kumozaki et al., 2015; Liang et al., 2014), predict glycosylation sites (Caragea et al., 2007; Li et al., 2015; Taherzadeh et al., 2019; Pitti et al., 2019), and classify glycans (Yamanishi et al., 2007). Alongside the advancements in deep learning, recent models have showcased the potential of deep learning in addressing glycomics challenges. Some approaches utilize sequence-based models, such as DeepNGlyPred (Pakhrin et al., 2021) that employs the N-GlyDE dataset (Pitti et al., 2019) to identify N-glycosylated sequons. Other sequence-based models like SweetOrigins (Bojar et al., 2020b), SweetTalk (Bojar et al., 2020a), and glyBERT (Dai et al., 2021) have utilized databases such as SugarBase (Bojar et al., 2020b) to predict various glycan properties. On another line of research, SweetNet (Burkholz et al., 2021), LectinOracle (Lundstrøm et al., 2022), GlyNet (Carpenter et al., 2022) and GNNGLY (Alkuhlani et al., 2023) represent glycans as graphs with monosaccharides as their nodes and use graph neural networks (GNNs) for glycan property prediction. Among all, GlycanML (Xu et al., 2024) established a comprehensive benchmark evaluating sequence-based models and GNNs on a diverse set of 11 tasks.

While GNNs have demonstrated their strong performance on specific tasks (Xu et al., 2024), their potential remains constrained by the underutilization of atomic-level information. Moreover, atomic-level encoders originally designed for small molecules have been shown to be ineffective in glycan modeling (Xu et al., 2024). In this study, we tackle these limitations by proposing the GlycanAA model, a hierarchical encoder for heterogeneous all-atom glycan graphs.

Self-Supervised Pre-training (SSP) in the biological domain. SSP has emerged as a powerful approach in deep learning, greatly improving the ability to learn informative and transferable representations from large-scale unlabeled data (Devlin, 2018; He et al., 2020). SSP enables models to generalize better across various tasks while reducing the need for extensive labeled data.

In recent years, SSP has also gained remarkable success in the biological domain, where the availability of large-scale biological datasets makes pre-training techniques well-suited. For small molecules, SSP has improved molecular representations, facilitating tasks like molecular property prediction and drug discovery (Hu et al., 2019; Xia et al., 2022). Protein modeling is similarly benefited, with methods like protein language modeling (Madani et al., 2020; Elnaggar et al., 2021;

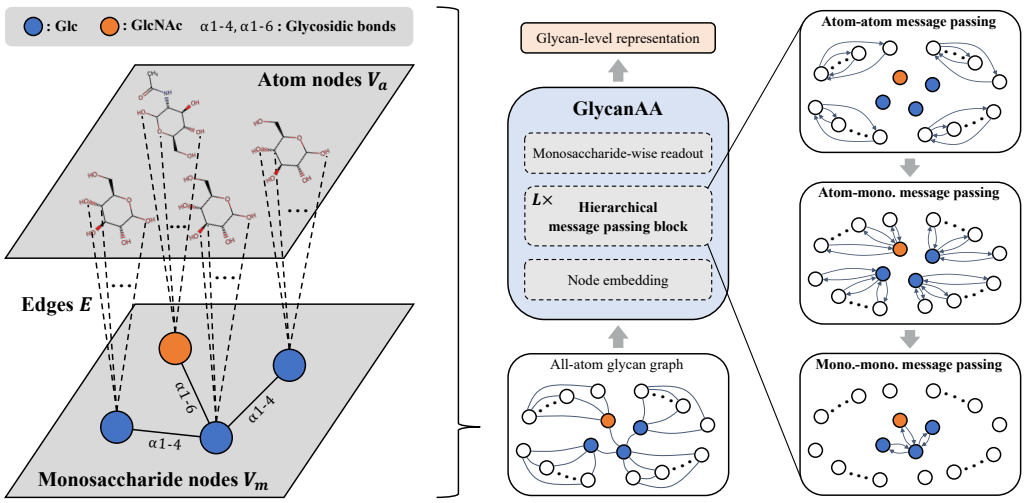

(a) All-Atom Glycan Graph **(b) GlycanAA with Hierarchical Message Passing**

Figure 1: *Illustration of GlycanAA.* (a) GlycanAA represents a glycan as an all-atom heterogeneous graph with atom nodes, monosaccharide nodes and different types of edges between these nodes. (b) Based on such a graph, GlycanAA models atom-atom, atom-monosaccharide and monosaccharide-monosaccharide interactions through hierarchical message passing. *Abbr.*, Glc: Glucose, GlcNAc: N-Acetylglucosamine, mono.: monosaccharide.

Rives et al., 2021; Lin et al., 2022; Hayes et al., 2024), geometric structure pre-training (Zhang et al., 2023b; 2024) and multimodal approaches (Xu et al., 2023; Duy Nguyen & Son Hy, 2024). In DNA research, models like DNABERT (Ji et al., 2021) and DNAGPT (Zhang et al., 2023a) have successfully applied Transformer models to DNA sequences, improving downstream analysis. RNA studies have also seen progresses, with models such as GenerRNA (Zhao et al., 2024) and UNI-RNA (Wang et al., 2023) employing pre-training to improve RNA sequence understanding.

Despite these advances, the potential of SSP in glycan modeling remains largely unexplored, presenting a new area of opportunity. In this work, we fill this gap by introducing the PreGlycanAA model which performs multi-scale pre-training on a high-quality unlabeled glycan dataset, leading to performance gains on various downstream glycan understanding tasks.

3 GlycanAA: All-Atom Glycan Modeling with Hierarchical Message Passing

We propose the GlycanAA model for all-atom-wise glycan modeling. In the following parts, we introduce its data representation method in Section 3.1 and its encoding approach in Section 3.2.

3.1 Heterogeneous Graph Representation of All-Atom Glycan Structure

For a glycan g, we represent its atomic-level structure as a heterogeneous graph $g = (\mathcal{V}_a, \mathcal{V}_m, \mathcal{E})$ composed of an atom node set $\mathcal{V}_a$, a monosaccharide node set $\mathcal{V}_m$ and an edge set $\mathcal{E}$, as graphically illustrated in Figure 1(a). We state the details of each graph component as below:

- **Atom node set** $\mathcal{V}_a$: This node set contains all heavy atoms (*i.e.*, non-hydrogen atoms) in a glycan, *i.e.*, $\mathcal{V}_a = \{a_i\}_{i=1}^{N}$ (a_i stands for an atom; N denotes the number of atoms in glycan g).
- **Monosaccharide node set** $\mathcal{V}_m$: To clearly represent the backbone structure of a glycan, we further introduce a set of nodes representing all monosaccharides that make up the glycan, *i.e.*, $\mathcal{V}_m = \{m_j\}_{j=1}^{M}$ (m_j stands for a monosaccharide; M denotes the number of monosaccharides in glycan g).
- **Edge set** $\mathcal{E}$: We consider three kinds of edges to comprehensively represent atom-atom, atom-monosaccharide and monosaccharide-monosaccharide interactions, *i.e.*, $\mathcal{E} = \mathcal{E}_{aa} \cup \mathcal{E}_{am} \cup \mathcal{E}_{mm}$, as detailed below:

- *Atom-atom edge set* $\mathcal{E}_{aa}$: This set of edges represent the atomic-level structure of each monosaccharide. Specifically, the covalent bonds in each monosaccharide are collected, and each bond along with its bond type (single, double, triple or aromatic bond) makes up an edge, *i.e.*, $\mathcal{E}_{aa} = \{(a, a', r) | r \in \{\text{single}, \text{double}, \text{triple}, \text{aromatic}\}\}$, where (a, a', r) denotes an edge connecting atom a to atom a' with bond type r. We include both directions of a bond in this edge set.
- *Atom-monosaccharide edge set* $\mathcal{E}_{am}$: We connect each atom with its corresponding monosaccharide, such that a monosaccharide is aware of its atomic-level information, and each atom recognizes the glycan backbone structure. This edge set is represented as $\mathcal{E}_{am} = \{(a, m, r_{am})\} \cup \{(m, a, r_{am})\}$, where each corresponding pair of atom a and monosaccharide m are connected by a bidirectional edge with the edge type r_{am} indicating atom-monosaccharide interaction.
- *Monosaccharide-monosaccharide edge set* $\mathcal{E}_{mm}$: We collect all glycosidic bonds in a glycan to represent its backbone structure. In specific, this edge set can be represented as $\mathcal{E}_{mm} = \{(m, m', r) | r \in \mathcal{R}_g\}$, where (m, m', r) denotes an edge connecting monosaccharide m to monosaccharide m' with bond type r, and $\mathcal{R}_g$ denotes all possible types of glycosidic bonds, *e.g.*, alpha-1,6-glycosidic bond, beta-1,4-glycosidic bond, *etc.* We follow Thomès et al. (2021) to construct $\mathcal{R}_g$ and include both directions of a bond in this edge set.

3.2 Hierarchical Message Passing on All-Atom Glycan Graph

Based on the all-atom glycan graph introduced above, GlycanAA extracts glycan representations using the carefully-designed modules below. A graphical illustration is shown in Figure 1(b).

Node embedding: We employ two codebooks to store the embeddings of all possible types of atoms and monosaccharides, respectively. For each node, we look up the corresponding codebook to assign it an initial feature embedding.

Hierarchical message passing: A glycan possesses a hierarchical structure, where its local structure in each monosaccharide is formed by atoms and covalent bonds in between, and different monosaccharides are further connected by glycosidic bonds, deriving its global backbone structure. We propose to encode such a structure from local to global hierarchically, which is proven to be effective in modeling other biomolecules like small molecules (Yu & Gao, 2022; Han et al., 2023) and proteins (Hermosilla et al., 2020; Wang et al., 2022). Specifically, in each message passing block, we sequentially perform atom-atom, atom-monosaccharide and monosaccharide-monosaccharide message passing to capture from local interactions to global interactions.

Note that, these interactions are essentially *multi-relational*, where atoms and monosaccharides interact with different types of covalent and glycosidic bonds. To fully model such interactions, we adopt relational graph convolution (RGConv) (Schlichtkrull et al., 2018) as the basic message passing module. Given a graph $g_0 = (\mathcal{V}_0, \mathcal{E}_0, \mathcal{R}_0)$ with node set $\mathcal{V}_0$, edge set $\mathcal{E}_0$ and relation (*i.e.*, edge type) set $\mathcal{R}_0$, RGConv updates node representations $Z_0 = \{z_i\}_{i=1}^{|\mathcal{V}_0|}$ by aggregating neighborhood information with per-relation convolutional operations:

$$\begin{aligned} Z_0' = \{z_i'\}_{i=1}^{|\mathcal{V}_0|} &= \mathrm{RGConv}(Z_0; \mathcal{V}_0, \mathcal{E}_0, \mathcal{R}_0), \\ \text{with} \;\; z_i' &= W_{\text{self}}\, z_i + \sigma\left(\mathrm{BN}\left(\sum_{r \in \mathcal{R}_0} \sum_{v_j \in \mathcal{N}_r(v_i)} \frac{1}{|\mathcal{N}_r(v_i)|} W_r z_j\right)\right), \end{aligned} \tag{1}$$

where Z_0' denotes the updated node representations, $\mathcal{N}_r(v_i) = \{v_j | (v_j, v_i, r) \in \mathcal{E}_0\}$ are the neighbors of node v_i with relation r, W_r denotes the convolutional kernel matrix for relation r, and W_{self} is the weight matrix for self-update. Here BN denotes a batch normalization layer, and we use a ReLU function as the activation $\sigma(\cdot)$.

Based on RGConv, we perform hierarchical message passing in three steps as below:

Atom-atom message passing: $Z_a' = \mathrm{RGConv}(Z_a; \mathcal{V}_a, \mathcal{E}_{aa}, \mathcal{R}_{aa}),$ (2)

Atom-mono. message passing: $(Z_a'', Z_m') = \mathrm{RGConv}\big((Z_a', Z_m); \mathcal{V}_a \cup \mathcal{V}_m, \mathcal{E}_{am}, \mathcal{R}_{am}\big),$ (3)

Mono.-mono. message passing: $Z_m'' = \mathrm{RGConv}(Z_m'; \mathcal{V}_m, \mathcal{E}_{mm}, \mathcal{R}_{mm}),$ (4)

where $\mathcal{R}_{aa}$ contains all types of covalent bonds, $\mathcal{R}_{am}$ stores the relation of atom-monosaccharide interaction, $\mathcal{R}_{mm}$ contains all types of glycosidic bonds, and "mono." is the abbreviation of monosaccharide. In this hierarchical process, atom representations Z_a are first updated to Z'_a by atom-atom message passing; atom and monosaccharide representations are then updated to Z''_a and Z'_m via atom-monosaccharide message passing; finally, monosaccharide representations are updated to Z''_m by monosaccharide-monosaccharide message passing.

Monosaccharide-wise readout: After L blocks of hierarchical message passing, we get the final atom representations Z_a^L and monosaccharide representations Z_m^L. We perform readout over all monosaccharide nodes to get a glycan-level representation: $z_g = [\mathrm{mean}(Z_m^L), \max(Z_m^L)]$, where $\mathrm{mean}(\cdot)$ and $\max(\cdot)$ denote mean and max pooling, respectively, and $[\cdot,\cdot]$ stands for concatenation. We exclude atom nodes in the readout, considering that (1) many monosaccharides share similar or even the same atomic structure, leading to duplicating information in representation readout, and (2) useful atomic information has already been passed to monosaccharide nodes during atom-monosaccharide message passing. The ablation study in Section 5.3 also supports the superiority of monosaccharide-wise readout over all-node readout.

4 PreGlycanAA: Pre-train All-Atom Glycan Representations with Multi-Scale Mask Prediction

To further improve the representation power of GlycanAA, we endow it with the knowledge stored in abundant unlabeled glycan data through self-supervised pre-training, deriving the PreGlycanAA model. In the following parts, we introduce the setup of the pre-training dataset in Section 4.1 and the multi-scale pre-training algorithm in Section 4.2.

4.1 Curation of High-quality Unlabeled Glycan Dataset

To ensure the quality of pre-trained model, we aim to collect as much informative and clean glycan data as possible. We choose the GlyTouCan database (Tiemeyer et al., 2017) as the data source for its high recognition in the glycoscience domain and instant update of the latest glycan structures. We first collect all the glycans deposited in GlyTouCan, summing up to 219,857 glycans. Data cleaning is then performed based on the following criteria:

- **Data quality**: We discard all the glycans whose structures are not fully solved. In specific, if there is any monosaccharide or glycosidic bond with an undetermined type in a glycan, we regard it as a low-quality sample and remove it from pre-training.
- **Data integrity**: We preserve the glycan structures with a single connected component. Those samples with multiple components are discarded, so as to focus on learning the interactions within a single glycan structure.
- **Without data leakage**: We remove the glycans that occur in the dataset of any downstream task used in our experiments, so as to prevent data leakage during pre-training.

After such a filtering process, we preserve a set of 40,781 high-quality, integral and data-leakage-proof glycan samples for pre-training.

4.2 Self-Supervised Pre-training via Multi-Scale Mask Prediction

To acquire the rich information underlying the curated unlabeled glycan dataset, we propose the PreGlycanAA model that pre-trains GlycanAA with a multi-scale mask prediction task, as illustrated in Figure 2. This algorithm endows the model with knowledge about the dependencies between different atoms and monosaccharides in a glycan, realized by the following schemes.

Multi-scale masking: During pre-training, it is desired to simultaneously acquire atom-atom, atom-monosaccharide and monosaccharide-monosaccharide dependencies. To achieve this goal, in an all-atom glycan graph (Section 3.1), we mask partial atom nodes and partial monosaccharide nodes, and the model is asked to recover these masked nodes by leveraging their neighboring atoms and monosaccharides. The two-scale masking is performed as below:

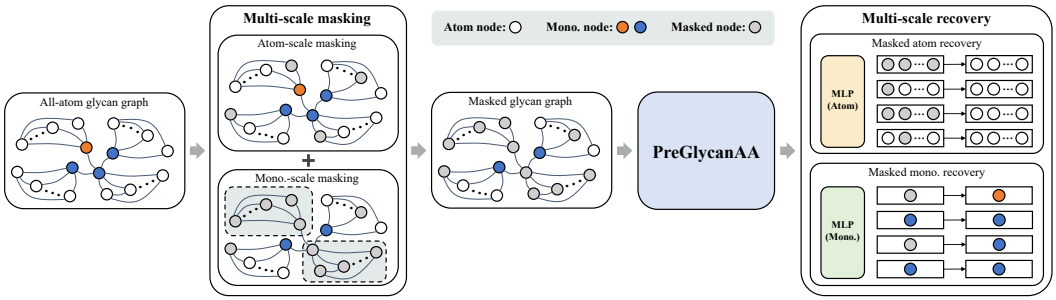

Figure 2: *Illustration of PreGlycanAA.* Upon an all-atom glycan graph, multi-scale masking derives a masked glycan graph with partially masked atoms and monosaccharides; PreGlycanAA learns multi-scale recovery to recover the complete glycan graph. *Abbr.*, mono.: monosaccharide.

- *Atom-scale masking*: For all heavy atoms in a glycan, we randomly select a part of them with the ratio ρ_a, and they are represented by a type of `Unknown-Atom`.
- *Monosaccharide-scale masking*: We select partial monosaccharides in a glycan with the ratio ρ_m. On one hand, their corresponding monosaccharide nodes in the graph are masked with a type of `Unknown-Monosaccharide`. On other hand, to avoid the trivial prediction of a masked monosaccharide based on some of its characteristic atoms, we further mask all atom nodes corresponding to the selected monosaccharides with the `Unknown-Atom` type.

Multi-scale recovery: The PreGlycanAA model learns to recover all these masked nodes. Specifically, for a masked glycan graph $\tilde{g}$, the model first extracts its atom and monosaccharide representations $\widetilde{Z}_a = \{\tilde{z}_a | a \in \mathcal{V}_a\}$ and $\widetilde{Z}_m = \{\tilde{z}_m | m \in \mathcal{V}_m\}$ through hierarchical message passing. Based on such representations with rich neighborhood information, two MLP predictors F_a and F_m are respectively employed to recover masked atoms and monosaccharides, deriving the following pre-training loss:

$$\mathcal{L}_{\text{pretrain}} = \frac{1}{|\mathcal{V}_a^{\text{mask}}| + |\mathcal{V}_m^{\text{mask}}|} \left(\sum_{a \in \mathcal{V}_a^{\text{mask}}} \mathcal{L}_{\text{CE}}\big(F_a(\tilde{z}_a), y_a\big) + \sum_{m \in \mathcal{V}_m^{\text{mask}}} \mathcal{L}_{\text{CE}}\big(F_m(\tilde{z}_m), y_m\big) \right), \quad (5)$$

where $\mathcal{V}_a^{\text{mask}}$ and $\mathcal{V}_m^{\text{mask}}$ denote the set of masked atom nodes and masked monosaccharide nodes, y_a and y_m represent the ground-truth type of a masked atom node a and a masked monosaccharide node m, and L_{CE} stands for the cross-entropy loss. In summary, this pre-training method encourages the model to capture different levels of dependencies in a glycan by solving a glycan recovery problem.

5 Experiments

5.1 Experimental Setups

Benchmark tasks: We evaluate the effectiveness of the proposed models on the GlycanML benchmark (Xu et al., 2024). This benchmark contains a comprehensive set of 11 glycan property and function prediction tasks, including glycan taxonomy prediction, glycan immunogenicity prediction, glycosylation type prediction and protein-glycan interaction prediction. Readers are referred to the original paper for detailed task descriptions and dataset statistics.

Model setups: For the sake of fair comparison with other baseline models in the GlycanML benchmark, both GlycanAA and PreGlycanAA are equipped with 3 hierarchical message passing blocks. During the pre-training phase of PreGlycanAA, both the masked atom predictor and the masked monosaccharide predictor are implemented as an MLP with 2 linear layers and a ReLU nonlinearity in between. For each benchmark task, we follow Xu et al. (2024) to perform task prediction with a 2-layer MLP with ReLU activation. In protein-glycan interaction prediction, the ESM-1b pre-trained protein language model (Rives et al., 2021) with fixed model parameters is used to extract protein representations. All implementations are based on the PyTorch deep learning library (Paszke et al., 2019) and TorchDrug drug discovery platform (Zhu et al., 2022).

Table 1: Benchmark results on GlycanML. We report *mean (std)* for each experiment. The best, second-best, and third-best performances are denoted by **bold**, underline, and *italic*, respectively. *Abbr.*, Immuno.: Immunogenicity; Glycos.: Glycosylation; GlycanAA-SP: GlycanAA with a single message passing in each block; GlycanAA-AN: GlycanAA with all-node readout.

Model	Taxonomy prediction								Immuno. (*AUPRC*)	Glycos. (*Macro-F1*)	Interaction (*Spearman's ρ*)	Weighted Mean Rank
	Domain (*Macro-F1*)	Kingdom (*Macro-F1*)	Phylum (*Macro-F1*)	Class (*Macro-F1*)	Order (*Macro-F1*)	Family (*Macro-F1*)	Genus (*Macro-F1*)	Species (*Macro-F1*)				
Monosaccharide-level Glycan Sequence Encoders												
Transformer	$0.612_{(0.009)}$	$0.546_{(0.079)}$	$0.316_{(0.014)}$	$0.235_{(0.022)}$	$0.147_{(0.007)}$	$0.114_{(0.039)}$	$0.065_{(0.001)}$	$0.047_{(0.008)}$	$\underline{0.856_{(0.012)}}$	$0.729_{(0.069)}$	$0.244_{(0.009)}$	15.34
Shallow CNN	$0.629_{(0.005)}$	$0.559_{(0.024)}$	$0.388_{(0.024)}$	$0.342_{(0.020)}$	$0.238_{(0.016)}$	$0.200_{(0.014)}$	$0.149_{(0.009)}$	$0.115_{(0.008)}$	$0.776_{(0.027)}$	$0.898_{(0.009)}$	$0.261_{(0.008)}$	11.88
LSTM	$0.621_{(0.012)}$	$0.566_{(0.076)}$	$0.413_{(0.036)}$	$0.272_{(0.029)}$	$0.174_{(0.023)}$	$0.145_{(0.012)}$	$0.098_{(0.016)}$	$0.078_{(0.008)}$	$\mathbf{0.912_{(0.068)}}$	$0.862_{(0.016)}$	$\mathit{0.280_{(0.001)}}$	10.5
ResNet	$0.635_{(0.009)}$	$0.505_{(0.025)}$	$0.331_{(0.061)}$	$0.301_{(0.010)}$	$0.183_{(0.082)}$	$0.165_{(0.019)}$	$0.112_{(0.018)}$	$0.073_{(0.007)}$	$0.754_{(0.124)}$	$0.919_{(0.004)}$	$0.273_{(0.004)}$	11.38
Monosaccharide-level Glycan Graph Encoders												
MPNN	$0.632_{(0.007)}$	$0.638_{(0.050)}$	$0.372_{(0.019)}$	$0.326_{(0.015)}$	$0.235_{(0.046)}$	$0.161_{(0.004)}$	$0.136_{(0.008)}$	$0.104_{(0.009)}$	$0.674_{(0.119)}$	$0.910_{(0.006)}$	$0.217_{(0.002)}$	17.41
GCN	$0.635_{(0.001)}$	$0.527_{(0.006)}$	$0.325_{(0.024)}$	$0.237_{(0.009)}$	$0.147_{(0.005)}$	$0.112_{(0.010)}$	$0.095_{(0.009)}$	$0.080_{(0.006)}$	$0.688_{(0.023)}$	$0.914_{(0.011)}$	$0.233_{(0.009)}$	17.41
GAT	$0.636_{(0.003)}$	$0.523_{(0.007)}$	$0.301_{(0.014)}$	$0.265_{(0.012)}$	$0.190_{(0.009)}$	$0.130_{(0.005)}$	$0.125_{(0.010)}$	$0.103_{(0.009)}$	$0.685_{(0.053)}$	$0.934_{(0.038)}$	$0.229_{(0.002)}$	16.22
GIN	$0.632_{(0.004)}$	$0.525_{(0.007)}$	$0.322_{(0.046)}$	$0.300_{(0.027)}$	$0.179_{(0.002)}$	$0.152_{(0.005)}$	$0.116_{(0.022)}$	$0.105_{(0.011)}$	$0.716_{(0.051)}$	$0.924_{(0.013)}$	$0.249_{(0.004)}$	14.09
CompGCN	$0.629_{(0.004)}$	$0.568_{(0.047)}$	$0.410_{(0.013)}$	$0.381_{(0.024)}$	$0.226_{(0.011)}$	$0.193_{(0.012)}$	$0.166_{(0.009)}$	$0.138_{(0.014)}$	$0.692_{(0.006)}$	$0.945_{(0.002)}$	$0.257_{(0.004)}$	11.59
RGCN	$0.633_{(0.001)}$	$0.647_{(0.054)}$	$\underline{0.462_{(0.033)}}$	$0.373_{(0.036)}$	$0.251_{(0.012)}$	$0.203_{(0.008)}$	$0.164_{(0.003)}$	$0.146_{(0.004)}$	$0.780_{(0.006)}$	$\mathit{0.948_{(0.004)}}$	$0.262_{(0.005)}$	6.47
PreRGCN	$0.636_{(0.005)}$	$0.664_{(0.032)}$	$0.451_{(0.023)}$	$0.389_{(0.016)}$	$0.265_{(0.015)}$	$\mathit{0.205_{(0.006)}}$	$0.172_{(0.010)}$	$0.139_{(0.008)}$	$0.781_{(0.019)}$	$\underline{0.949_{(0.015)}}$	$0.263_{(0.018)}$	*4.84*
GearNet	$0.471_{(0.005)}$	$0.577_{(0.036)}$	$0.395_{(0.025)}$	$0.389_{(0.010)}$	$0.256_{(0.007)}$	$0.189_{(0.004)}$	$0.165_{(0.003)}$	$0.136_{(0.003)}$	$0.740_{(0.015)}$	$0.892_{(0.027)}$	$0.248_{(0.004)}$	14.78
GearNet-Edge	$0.628_{(0.009)}$	$0.573_{(0.030)}$	$0.396_{(0.010)}$	$0.384_{(0.010)}$	$0.262_{(0.006)}$	$0.200_{(0.010)}$	$0.177_{(0.008)}$	$0.140_{(0.005)}$	$0.768_{(0.023)}$	$0.909_{(0.010)}$	$0.250_{(0.003)}$	11.44
All-Atom Glycan Encoders												
All-Atom RGCN	$0.637_{(0.001)}$	$0.624_{(0.007)}$	$0.293_{(0.014)}$	$0.156_{(0.028)}$	$0.112_{(0.023)}$	$0.096_{(0.006)}$	$0.063_{(0.007)}$	$0.035_{(0.005)}$	$0.520_{(0.017)}$	$0.928_{(0.017)}$	$0.215_{(0.003)}$	18.94
Graphormer	$\underline{0.640_{(0.006)}}$	$0.468_{(0.054)}$	$0.249_{(0.041)}$	$0.201_{(0.013)}$	$0.142_{(0.019)}$	$0.112_{(0.009)}$	$0.077_{(0.006)}$	$0.054_{(0.044)}$	$0.637_{(0.062)}$	$0.856_{(0.009)}$	$0.211_{(0.027)}$	21.91
GraphGPS	$0.477_{(0.002)}$	$0.511_{(0.040)}$	$0.314_{(0.022)}$	$0.261_{(0.051)}$	$0.153_{(0.018)}$	$0.134_{(0.008)}$	$0.105_{(0.006)}$	$0.065_{(0.017)}$	$0.637_{(0.075)}$	$0.883_{(0.032)}$	$0.247_{(0.016)}$	19.38
Uni-Mol+	$\mathit{0.639_{(0.004)}}$	$0.446_{(0.034)}$	$0.227_{(0.023)}$	$0.174_{(0.019)}$	$0.128_{(0.020)}$	$0.109_{(0.017)}$	$0.077_{(0.012)}$	$0.056_{(0.003)}$	$\mathit{0.789_{(0.099)}}$	$0.885_{(0.045)}$	$0.241_{(0.007)}$	15.34
GlycanAA-SP	$0.589_{(0.073)}$	$0.635_{(0.078)}$	$0.444_{(0.019)}$	$0.395_{(0.009)}$	$\underline{0.270_{(0.006)}}$	$\mathit{0.205_{(0.005)}}$	$0.176_{(0.015)}$	$\mathit{0.154_{(0.009)}}$	$0.755_{(0.010)}$	$0.946_{(0.017)}$	$0.241_{(0.003)}$	10.41
GlycanAA-AN	$0.609_{(0.028)}$	$\mathbf{0.688_{(0.002)}}$	$0.453_{(0.037)}$	$\mathbf{0.427_{(0.027)}}$	$\underline{0.270_{(0.009)}}$	$0.199_{(0.012)}$	$0.179_{(0.007)}$	$\mathbf{0.161_{(0.008)}}$	$0.765_{(0.024)}$	$0.947_{(0.025)}$	$0.241_{(0.004)}$	9.44
GlycanAA	$\mathbf{0.642_{(0.021)}}$	$\mathit{0.681_{(0.006)}}$	$0.455_{(0.022)}$	$\mathit{0.404_{(0.017)}}$	$\mathbf{0.278_{(0.014)}}$	$0.201_{(0.016)}$	$\mathit{0.186_{(0.020)}}$	$\mathit{0.154_{(0.007)}}$	$0.780_{(0.011)}$	$0.936_{(0.022)}$	$\underline{0.281_{(0.001)}}$	$\underline{4.66}$
Pre-trained All-Atom Glycan Encoders												
VabsNet	$0.607_{(0.004)}$	$0.622_{(0.022)}$	$0.363_{(0.006)}$	$0.261_{(0.023)}$	$0.175_{(0.015)}$	$0.125_{(0.003)}$	$0.104_{(0.005)}$	$0.068_{(0.006)}$	$0.742_{(0.040)}$	$0.903_{(0.015)}$	$0.160_{(0.008)}$	18.06
GlycanAA-Attribute	$0.628_{(0.007)}$	$\underline{0.687_{(0.001)}}$	$\mathit{0.457_{(0.028)}}$	$0.392_{(0.033)}$	$0.263_{(0.011)}$	$\underline{0.208_{(0.004)}}$	$\underline{0.188_{(0.001)}}$	$0.143_{(0.003)}$	$0.722_{(0.009)}$	$0.925_{(0.011)}$	$0.263_{(0.009)}$	9.88
GlycanAA-Context	$0.637_{(0.002)}$	$0.643_{(0.048)}$	$0.453_{(0.026)}$	$0.386_{(0.038)}$	$0.259_{(0.033)}$	$\mathit{0.205_{(0.005)}}$	$0.177_{(0.004)}$	$0.144_{(0.007)}$	$0.768_{(0.013)}$	$0.946_{(0.018)}$	$0.270_{(0.010)}$	6.56
PreGlycanAA	$\underline{0.640_{(0.002)}}$	$0.672_{(0.011)}$	$\mathbf{0.469_{(0.009)}}$	$\underline{0.406_{(0.003)}}$	$\mathit{0.267_{(0.005)}}$	$\mathbf{0.220_{(0.006)}}$	$\mathbf{0.190_{(0.007)}}$	$\underline{0.159_{(0.009)}}$	$0.782_{(0.019)}$	$\mathbf{0.953_{(0.008)}}$	$\mathbf{0.292_{(0.002)}}$	**2.06**

Pre-training setups: The PreGlycanAA model is pre-trained with an Adam optimizer (learning rate: 5×10^{-4}, weight decay: 1×10^{-3}, batch size: 256) for 50 epochs on the curated pre-training dataset (Section 4.1). We set both the atom mask ratio ρ_a and the monosaccharide mask ratio ρ_m as 0.3, and the sensitivities of these two parameters are analyzed in Section 5.3. We provide the accuracy and perplexity curves of pre-training in Appendix A.1. All pre-training experiments are conducted on a local server with 200 CPU cores and 10 NVIDIA GeForce RTX 4090 GPUs (24GB).

Downstream training setups: Following the standard of GlycanML benchmark, we conduct all experiments on seeds 0, 1 and 2 and report the mean and standard deviation of results. For GlycanAA, we train it with an Adam optimizer (learning rate: 5×10^{-4}, weight decay: 1×10^{-3}) for 50 epochs with batch size 256 on taxonomy, immunogenicity and glycosylation type prediction and for 10 epochs with batch size 32 on interaction prediction. For fine-tuning PreGlycanAA on downstream tasks, we keep other settings the same as GlycanAA except that the learning rate of the encoder part is set as one tenth of that of the following task-specific MLP predictor (*i.e.*, encoder learning rate: 5×10^{-5}, predictor learning rate: 5×10^{-4}). For model selection, we perform validation after each training epoch, and the checkpoint with the best validation performance is chosen for test. All downstream experiments are conducted on a local server with 100 CPU cores and 4 NVIDIA GeForce RTX 4090 GPUs (24GB).

5.2 Benchmark Results on GlycanML

Evaluation metrics: As in the original benchmark, we use Macro-F1 score as the metric for taxonomy and glycosylation type prediction, AUPRC as the metric for immunogenicity prediction, Spearman's ρ as the metric for interaction prediction, and weighted mean rank as the metric for a model's comprehensive performance. Weighted mean rank computes the weighted average of a model's ranks over all tasks, where each taxonomy prediction task weighs $1/8$ and each of the other three tasks weighs 1, such that the task number imbalance between different task types is eliminated.

Baselines: We compare our models with the baselines studied in the GlycanML benchmark (Xu et al., 2024), including four monosaccharide-level glycan sequence encoders (*i.e.*, LSTM (Hochreiter & Schmidhuber, 1997), ResNet (He et al., 2016), Transformer (Vaswani et al., 2017) and Shallow CNN (Shanehsazzadeh et al., 2020)), eight monosaccharide-level glycan graph encoders (GCN (Kipf & Welling, 2017), GAT (Veličković et al., 2017), MPNN (Gilmer et al., 2017), GIN (Xu

et al., 2018), CompGCN (Vashishth et al., 2019), RGCN (Schlichtkrull et al., 2018), GearNet (Zhang et al., 2023b) and GearNet-Edge (Zhang et al., 2023b)), four state-of-the-art all-atom molecular encoders (*i.e.*, Graphormer (Ying et al., 2021), GraphGPS (Rampášek et al., 2022), Uni-Mol+ (Lu et al., 2024) and VabsNet (Zhuang et al., 2024)). Given the strong performance of RGCN on modeling monosaccharide-level glycan graphs as shown in Xu et al. (2024), we additionally evaluate it on modeling the all-atom molecular graphs of glycans, namely All-Atom RGCN, and also pre-train it with a similar mask prediction algorithm as PreGlycanAA, namely PreRGCN. To study pre-training more in depth, we employ the pre-training methods, attribute masking and context prediction, proposed in Hu et al. (2019) to pre-train GlycanAA, deriving the GlycanAA-Attribute and GlycanAA-Context models to compare with PreGlycanAA.

Results: In Table 1, we report the performance of the proposed models and various baselines. Based on these results, we highlight the findings below:

- **The superiority of GlycanAA over existing glycan encoders illustrates the benefits of all-atom glycan modeling.** It is observed that GlycanAA outperforms the best baseline result on 7 out of 11 tasks and also surpasses all baselines in terms of weighted mean rank. Therefore, it is beneficial to utilize atomic-level information in addition to monosaccharide-level information, and the superiority of GlycanAA derives from well leveraging both kinds of information. Especially, GlycanAA also outperforms the PreRGCN model pre-trained with a similar approach as PreGlycanAA, which verifies the value of modeling glycans on the all-atom level and also illustrates the importance of hierarchical structures to our pre-training method.

- **The performance gains of PreGlycanAA over GlycanAA demonstrate the effectiveness of the proposed pre-training method.** PreGlycanAA outperforms GlycanAA on 8 out of 11 tasks and ranks first among all models in terms of weighted mean rank. Given the same model architecture between PreGlycanAA and GlycanAA, we confirm that the proposed multi-scale pre-training method can enhance the model capability.

  By comparison, both GlycanAA-Attribute and GlycanAA-Context models show performance decay compared to the GlycanAA model without pre-training. We suggest that these two pre-training methods actually lead to trivial tasks during pre-training, which mainly causes the negative results. Specifically, the attribute masking method does not consider the correlation between atom and monosaccharide nodes during masking, and thus leads to the trivial prediction of a masked monosaccharide based on some of its characteristic atoms; similarly, the context prediction method could select highly correlated center and anchor nodes in an all-atom glycan graph, leading to a trivial prediction task. By comparison, the proposed PreGlycanAA model performs multi-scale masking carefully to ensure as little correlation left in the unmasked nodes as possible, leading to clearly better performance than the GlycanAA without pre-training.

- **Directly applying performant small molecule encoders or monosaccharide-level glycan encoders to all-atom glycan modeling is unpromising.** Graphormer, GraphGPS and Uni-Mol+ have been shown to be effective in modeling small molecules with tens of atoms (Shi et al., 2022). However, benchmark results show that they do not perform well when modeling all-atom molecular graphs of glycans with hundreds of atoms. Similarly, compared to the well-performing monosaccharide-level RGCN, the performance of All-Atom RGCN is unsatisfactory. These results illustrate the necessity of dedicated design for all-atom glycan modeling.

5.3 Ablation Studies

Effect of hierarchical message passing: To study the necessity of hierarchical message passing, we substitute it with a single message passing in each message passing block of GlycanAA, where the single message passing is also implemented as relational graph convolution (Equation (1)). We name this model variant as GlycanAA-SP (*i.e.*, GlycanAA with a single message passing in each block). By comparing the performance of GlycanAA and GlycanAA-SP in Table 1, we can observe the obvious advantages of GlycanAA, where it achieves a better result on 8 out of 11 tasks, and it owns clearly better weighted mean rank (GlycanAA: 4.66 *v.s.* GlycanAA-SP: 10.41). These results demonstrate the benefit of passing messages hierarchically on the proposed all-atom glycan graph, where atom-atom, atom-monosaccharide and monosaccharide-monosaccharide interactions are separately modelled by different message passing modules, enhancing the model capacity.

Effect of monosaccharide-wise readout: In GlycanAA, we by default use monosaccharide-wise readout to derive glycan-level representations. Here, we compare this scheme with all-node readout, where mean and max pooling are performed over all atom and monosaccharide nodes, instead of just over monosaccharide nodes as in monosaccharide-wise readout. The model variant with all-node readout is named as GlycanAA-AN. According to the results in Table 1, GlycanAA shows superiority over GlycanAA-AN, where GlycanAA performs better on 7 out of 11 tasks, and its weighted mean rank is clearly higher (GlycanAA: 4.66 *v.s.* GlycanAA-AN: 9.44). Therefore, monosaccharide-wise readout is verified to be a better readout scheme. For all-atom readout, since many monosaccharides share similar or even the same atomic structure, much duplicating information is involved in glycan representations, which could make glycan representations less discriminative, leading to performance decay. By comparison, for monosaccharide-wise readout, glycan representations contain only useful atomic information that is passed to monosaccharide nodes during atom-monosaccharide message passing, leading to more discriminative glycan representations and thus better performance.

Sensitivity of PreGlycanAA to mask ratio: In this experiment, we analyze how different atom and monosaccharide mask ratios affect the performance of PreGlycanAA on downstream tasks. Specifically, we uniformly select atom and monosaccharide mask ratios between 0 and 1 with the interval of 0.15 and combine them into 36 pairs: $(\rho_a, \rho_m) \in \{0.15, 0.3, 0.45, 0.6, 0.75, 0.9\} \times \{0.15, 0.3, 0.45, 0.6, 0.75, 0.9\}$. We pre-train a model under each mask ratio pair and evaluate its performance on eight glycan taxonomy prediction tasks. In Figure 3, we visualize the average Macro-F1 score on eight taxonomy prediction tasks for 36 pre-trained models with different mask ratios. According to the results, it is observed that the pre-trained model achieves prominent performance when both the atom and monosaccharide mask ratio are around 0.3. Under such settings, a suitable balance is achieved between masked and observed information in a glycan, and therefore the model can be effectively pre-trained by the proposed multi-scale mask prediction algorithm.

Figure 3: Average Macro-F1 score of PreGlycanAA on eight taxonomy prediction tasks under different atom and monosaccharide mask ratios.

5.4 Computational Efficiency Study

To evaluate the additional computational cost brought by all-atom glycan modeling compared to monosaccharide-level modeling, we study the computational efficiency of GlycanAA against a typical monosaccharide-level glycan encoder, RGCN. Specifically, we evaluate their training and inference speed in terms of throughput (*i.e.*, the number of samples processed in one second) and their training and inference memory cost in terms of Mebibyte (MiB). The evaluation is performed on the dataset of glycan taxonomy prediction for its good coverage of different kinds of glycans (#training/validation/test samples: 11,010/1,280/919, average #monosaccharides per glycan: 6.39, minimum #monosaccharides per glycan: 2, maximum #monosaccharides per glycan: 43). All experiments are conducted on a machine with 32 CPU cores and 1 NVIDIA GeForce RTX 4090 GPU (24GB), and the batch size is set as 256 for both models.

Table 2: Efficiency comparison between RGCN and GlycanAA on taxonomy prediction dataset.

Model	Training speed (#samples / s)	Inference speed (#samples / s)	Training memory cost (MiB)	Inference memory cost (MiB)
RGCN	885.7	1486.9	6911.6	3563.5
GlycanAA	679.8	1158.6	8213.9	4251.2

In Table 2, we present the efficiency comparisons between RGCN and GlycanAA. It is observed that, in terms of both speed and memory cost, GlycanAA does not introduce too much extra cost compared to RGCN during both training and inference. Specifically, for training/inference speed, GlycanAA is about 22% slower than RGCN, and, for training/inference memory cost, GlycanAA consumes about 19% more memory than RGCN. Such a moderate extra cost brings the superior performance of GlycanAA over RGCN on 7 out of 11 benchmark tasks and also on the weighted mean rank (shown in Table 1), illustrating the "worth" of modeling glycans on the all-atom level.

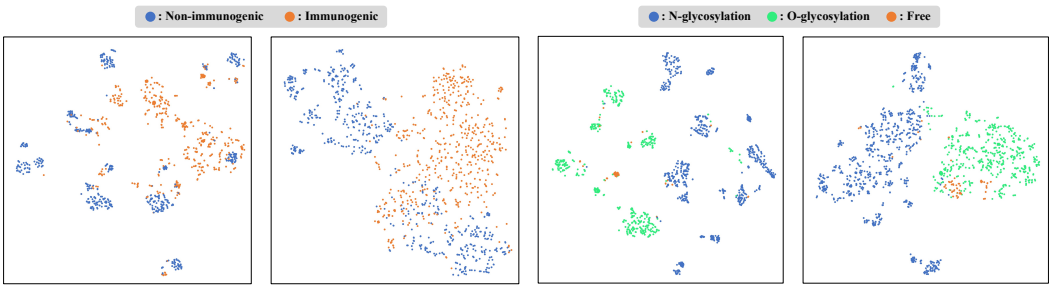

(a) Immuno. with Randomly-Initialized *GlycanAA* (b) Immuno. with Pre-trained *PreGlycanAA* (c) Glycos. with Randomly-Initialized *GlycanAA* (d) Glycos. with Pre-trained *PreGlycanAA*

Figure 4: Visualization of glycan representations extracted by GlycanAA and PreGlycanAA on downstream task datasets. *Abbr.*, Immuno.: Immunogenicity; Glycos.: Glycosylation.

5.5 Visualization

To intuitively assess the effectiveness of the proposed pre-training method, we visualize the glycan representations extracted by the GlycanAA model with randomly initialized weights and the PreGlycanAA model with pre-trained weights, respectively. We use the t-SNE algorithm (Van der Maaten & Hinton, 2008) to compress glycan representations to a two-dimensional space. The visualization results on the datasets of immunogenicity and glycosylation type prediction are presented in Figure 4, and the visualization results on other downstream tasks are shown in Appendix A.2.

According to the results in Figure 4, we observe that, after pre-training, the model can more effectively separate the samples of different classes and gather the samples of the same class together, leading to smoother decision boundaries. This effect leads to better generalization performance of PreGlycanAA over GlycanAA on immunogenicity and glycosylation type prediction tasks, as shown in Table 1. These visualization results provide a way to interpret how the proposed multi-scale pre-training method benefits downstream glycan understanding tasks.

6 Conclusions and Future Work

In this work, we aim to model all-atom-wise glycan structures. We first propose the GlycanAA model to encode heterogeneous all-atom glycan graphs. GlycanAA captures from local atomic-level interactions to global monosaccharide-level interactions with a carefully-designed hierarchical message passing scheme. To further enhance the representation power of GlycanAA, we pre-train it on a set of high-quality unlabeled glycans, deriving the PreGlycanAA model. During pre-training, the model learns to solve a multi-scale mask prediction task, which endows the model with knowledge about different levels of dependencies in a glycan. Through extensively evaluating the proposed models on the GlycanML benchmark, we illustrate the superior performance of GlycanAA over existing glycan encoders and verify the further improvements achieved by PreGlycanAA.

In the future, we will focus on boosting real-world glycan-related applications with the proposed models and their variants. For example, we will study how vaccine design and cancer research can be promoted by all-atom glycan machine learning models.

REFERENCES

Alhasan Alkuhlani, Walaa Gad, Mohamed Roushdy, and Abdel-Badeeh M Salem. Gnngly: Graph neural networks for glycan classification. *IEEE Access*, 2023.

Daniel Bojar and Frederique Lisacek. Glycoinformatics in the artificial intelligence era. *Chemical Reviews*, 122(20):15971–15988, 2022.

Daniel Bojar, Diogo M Camacho, and James J Collins. Using natural language processing to learn the grammar of glycans. *bioRxiv*, pp. 2020–01, 2020a.

Daniel Bojar, Rani K Powers, Diogo M Camacho, and James J Collins. Sweetorigins: Extracting evolutionary information from glycans. *bioRxiv*, pp. 2020–04, 2020b.

Rebekka Burkholz, John Quackenbush, and Daniel Bojar. Using graph convolutional neural networks to learn a representation for glycans. *Cell Reports*, 35(11), 2021.

Cornelia Caragea, Jivko Sinapov, Adrian Silvescu, Drena Dobbs, and Vasant Honavar. Glycosylation site prediction using ensembles of support vector machine classifiers. *BMC bioinformatics*, 8:1–13, 2007.

Eric J Carpenter, Shaurya Seth, Noel Yue, Russell Greiner, and Ratmir Derda. Glynet: a multi-task neural network for predicting protein–glycan interactions. *Chemical Science*, 13(22):6669–6686, 2022.

Bowen Dai, Daniel E Mattox, and Chris Bailey-Kellogg. Attention please: modeling global and local context in glycan structure-function relationships. *bioRxiv*, pp. 2021–10, 2021.

Jacob Devlin. Bert: Pre-training of deep bidirectional transformers for language understanding. *arXiv preprint arXiv:1810.04805*, 2018.

Viet Thanh Duy Nguyen and Truong Son Hy. Multimodal pretraining for unsupervised protein representation learning. *Biology Methods and Protocols*, pp. bpae043, 2024.

Ahmed Elnaggar, Michael Heinzinger, Christian Dallago, Ghalia Rehawi, Yu Wang, Llion Jones, Tom Gibbs, Tamas Feher, Christoph Angerer, Martin Steinegger, et al. Prottrans: Toward understanding the language of life through self-supervised learning. *IEEE transactions on pattern analysis and machine intelligence*, 44(10):7112–7127, 2021.

Justin Gilmer, Samuel S Schoenholz, Patrick F Riley, Oriol Vinyals, and George E Dahl. Neural message passing for quantum chemistry. In *International conference on machine learning*, pp. 1263–1272. PMLR, 2017.

Shen Han, Haitao Fu, Yuyang Wu, Ganglan Zhao, Zhenyu Song, Feng Huang, Zhongfei Zhang, Shichao Liu, and Wen Zhang. Himgnn: a novel hierarchical molecular graph representation learning framework for property prediction. *Briefings in Bioinformatics*, 24(5):bbad305, 2023.

Tomas Hayes, Roshan Rao, Halil Akin, Nicholas J Sofroniew, Deniz Oktay, Zeming Lin, Robert Verkuil, Vincent Q Tran, Jonathan Deaton, Marius Wiggert, et al. Simulating 500 million years of evolution with a language model. *bioRxiv*, pp. 2024–07, 2024.

Kaiming He, Xiangyu Zhang, Shaoqing Ren, and Jian Sun. Deep residual learning for image recognition. In *Proceedings of the IEEE conference on computer vision and pattern recognition*, pp. 770–778, 2016.

Kaiming He, Haoqi Fan, Yuxin Wu, Saining Xie, and Ross Girshick. Momentum contrast for unsupervised visual representation learning. In *Proceedings of the IEEE/CVF conference on computer vision and pattern recognition*, pp. 9729–9738, 2020.

Pedro Hermosilla, Marco Schäfer, Matěj Lang, Gloria Fackelmann, Pere Pau Vázquez, Barbora Kozlíková, Michael Krone, Tobias Ritschel, and Timo Ropinski. Intrinsic-extrinsic convolution and pooling for learning on 3d protein structures. *arXiv preprint arXiv:2007.06252*, 2020.

Sepp Hochreiter and Jürgen Schmidhuber. Long short-term memory. *Neural computation*, 9(8): 1735–1780, 1997.

Weihua Hu, Bowen Liu, Joseph Gomes, Marinka Zitnik, Percy Liang, Vijay Pande, and Jure Leskovec. Strategies for pre-training graph neural networks. *arXiv preprint arXiv:1905.12265*, 2019.

Yanrong Ji, Zhihan Zhou, Han Liu, and Ramana V Davuluri. Dnabert: pre-trained bidirectional encoder representations from transformers model for dna-language in genome. *Bioinformatics*, 37(15):2112–2120, 2021.

Thomas N Kipf and Max Welling. Semi-supervised classification with graph convolutional networks. *International Conference on Learning Representations*, 2017.

Shotaro Kumozaki, Kengo Sato, and Yasubumi Sakakibara. A machine learning based approach to de novo sequencing of glycans from tandem mass spectrometry spectrum. *IEEE/ACM transactions on computational biology and bioinformatics*, 12(6):1267–1274, 2015.

Ken S Lau, Emily A Partridge, Ani Grigorian, Cristina I Silvescu, Vernon N Reinhold, Michael Demetriou, and James W Dennis. Complex n-glycan number and degree of branching cooperate to regulate cell proliferation and differentiation. *Cell*, 129(1):123–134, 2007.

Fuyi Li, Chen Li, Mingjun Wang, Geoffrey I Webb, Yang Zhang, James C Whisstock, and Jiangning Song. Glycomine: a machine learning-based approach for predicting n-, c-and o-linked glycosylation in the human proteome. *Bioinformatics*, 31(9):1411–1419, 2015.

Haining Li, Austin WT Chiang, and Nathan E Lewis. Artificial intelligence in the analysis of glycosylation data. *Biotechnology Advances*, 60:108008, 2022.

Suh-Yuen Liang, Sz-Wei Wu, Tsung-Hsien Pu, Fang-Yu Chang, and Kay-Hooi Khoo. An adaptive workflow coupled with random forest algorithm to identify intact n-glycopeptides detected from mass spectrometry. *Bioinformatics*, 30(13):1908–1916, 2014.

Zeming Lin, Halil Akin, Roshan Rao, Brian Hie, Zhongkai Zhu, Wenting Lu, Allan dos Santos Costa, Maryam Fazel-Zarandi, Tom Sercu, Sal Candido, et al. Language models of protein sequences at the scale of evolution enable accurate structure prediction. *BioRxiv*, 2022:500902, 2022.

Ya-Juan Liu and Cheng Wang. A review of the regulatory mechanisms of extracellular vesicles-mediated intercellular communication. *Cell Communication and Signaling*, 21(1):77, 2023.

Shuqi Lu, Zhifeng Gao, Di He, Linfeng Zhang, and Guolin Ke. Data-driven quantum chemical property prediction leveraging 3d conformations with uni-mol+. *Nature communications*, 15(1): 7104, 2024.

Jon Lundstrøm, Emma Korhonen, Frédérique Lisacek, and Daniel Bojar. Lectinoracle: a generalizable deep learning model for lectin–glycan binding prediction. *Advanced Science*, 9(1):2103807, 2022.

Ali Madani, Bryan McCann, Nikhil Naik, Nitish Shirish Keskar, Namrata Anand, Raphael R Eguchi, Po-Ssu Huang, and Richard Socher. Progen: Language modeling for protein generation. *arXiv preprint arXiv:2004.03497*, 2020.

Subash C Pakhrin, Kiyoko F Aoki-Kinoshita, Doina Caragea, and Dukka B Kc. Deepnglypred: a deep neural network-based approach for human n-linked glycosylation site prediction. *Molecules*, 26(23):7314, 2021.

Adam Paszke, Sam Gross, Francisco Massa, Adam Lerer, James Bradbury, Gregory Chanan, Trevor Killeen, Zeming Lin, Natalia Gimelshein, Luca Antiga, et al. Pytorch: An imperative style, high-performance deep learning library. *Advances in neural information processing systems*, 32, 2019.

Thejkiran Pitti, Ching-Tai Chen, Hsin-Nan Lin, Wai-Kok Choong, Wen-Lian Hsu, and Ting-Yi Sung. N-glyde: a two-stage n-linked glycosylation site prediction incorporating gapped dipeptides and pattern-based encoding. *Scientific reports*, 9(1):15975, 2019.

Ladislav Rampášek, Michael Galkin, Vijay Prakash Dwivedi, Anh Tuan Luu, Guy Wolf, and Dominique Beaini. Recipe for a general, powerful, scalable graph transformer. *Advances in Neural Information Processing Systems*, 35:14501–14515, 2022.

Alexander Rives, Joshua Meier, Tom Sercu, Siddharth Goyal, Zeming Lin, Jason Liu, Demi Guo, Myle Ott, C Lawrence Zitnick, Jerry Ma, et al. Biological structure and function emerge from scaling unsupervised learning to 250 million protein sequences. *Proceedings of the National Academy of Sciences*, 118(15):e2016239118, 2021.

Michael Schlichtkrull, Thomas N Kipf, Peter Bloem, Rianne Van Den Berg, Ivan Titov, and Max Welling. Modeling relational data with graph convolutional networks. In *The semantic web: 15th international conference, ESWC 2018, Heraklion, Crete, Greece, June 3–7, 2018, proceedings 15*, pp. 593–607. Springer, 2018.

Amir Shanehsazzadeh, David Belanger, and David Dohan. Is transfer learning necessary for protein landscape prediction? *arXiv preprint arXiv:2011.03443*, 2020.

Yu Shi, Shuxin Zheng, Guolin Ke, Yifei Shen, Jiacheng You, Jiyan He, Shengjie Luo, Chang Liu, Di He, and Tie-Yan Liu. Benchmarking graphormer on large-scale molecular modeling datasets. *arXiv preprint arXiv:2203.04810*, 2022.

Ghazaleh Taherzadeh, Abdollah Dehzangi, Maryam Golchin, Yaoqi Zhou, and Matthew P Campbell. Sprint-gly: predicting n-and o-linked glycosylation sites of human and mouse proteins by using sequence and predicted structural properties. *Bioinformatics*, 35(20):4140–4146, 2019.

Luc Thomès, Rebekka Burkholz, and Daniel Bojar. Glycowork: A python package for glycan data science and machine learning. *Glycobiology*, 31(10):1240–1244, 2021.

Michael Tiemeyer, Kazuhiro Aoki, James Paulson, Richard D Cummings, William S York, Niclas G Karlsson, Frederique Lisacek, Nicolle H Packer, Matthew P Campbell, Nobuyuki P Aoki, et al. Glytoucan: an accessible glycan structure repository. *Glycobiology*, 27(10):915–919, 2017.

Laurens Van der Maaten and Geoffrey Hinton. Visualizing data using t-sne. *Journal of machine learning research*, 9(11), 2008.

Shikhar Vashishth, Soumya Sanyal, Vikram Nitin, and Partha Talukdar. Composition-based multi-relational graph convolutional networks. *arXiv preprint arXiv:1911.03082*, 2019.

Ashish Vaswani, Noam Shazeer, Niki Parmar, Jakob Uszkoreit, Llion Jones, Aidan N Gomez, Łukasz Kaiser, and Illia Polosukhin. Attention is all you need. *Advances in neural information processing systems*, 30, 2017.

Petar Veličković, Guillem Cucurull, Arantxa Casanova, Adriana Romero, Pietro Lio, and Yoshua Bengio. Graph attention networks. *arXiv preprint arXiv:1710.10903*, 2017.

Limei Wang, Haoran Liu, Yi Liu, Jerry Kurtin, and Shuiwang Ji. Learning hierarchical protein representations via complete 3d graph networks. *arXiv preprint arXiv:2207.12600*, 2022.

Xi Wang, Ruichu Gu, Zhiyuan Chen, Yongge Li, Xiaohong Ji, Guolin Ke, and Han Wen. Uni-rna: universal pre-trained models revolutionize rna research. *bioRxiv*, pp. 2023–07, 2023.

Jun Xia, Yanqiao Zhu, Yuanqi Du, and Stan Z Li. A systematic survey of chemical pre-trained models. *arXiv preprint arXiv:2210.16484*, 2022.

Keyulu Xu, Weihua Hu, Jure Leskovec, and Stefanie Jegelka. How powerful are graph neural networks? *arXiv preprint arXiv:1810.00826*, 2018.

Minghao Xu, Xinyu Yuan, Santiago Miret, and Jian Tang. Protst: Multi-modality learning of protein sequences and biomedical texts. In *International Conference on Machine Learning*, pp. 38749–38767. PMLR, 2023.

Minghao Xu, Yunteng Geng, Yihang Zhang, Ling Yang, Jian Tang, and Wentao Zhang. Glycanml: A multi-task and multi-structure benchmark for glycan machine learning. *arXiv preprint arXiv:2405.16206*, 2024.

Issaku Yamada, Masaaki Shiota, Daisuke Shinmachi, Tamiko Ono, Shinichiro Tsuchiya, Masae Hosoda, Akihiro Fujita, Nobuyuki P Aoki, Yu Watanabe, Noriaki Fujita, et al. The glycosmos portal: a unified and comprehensive web resource for the glycosciences. *Nature Methods*, 17(7): 649–650, 2020.

Yoshihiro Yamanishi, Francis Bach, and Jean-Philippe Vert. Glycan classification with tree kernels. *Bioinformatics*, 23(10):1211–1216, 2007.

Masaki Yanagishita. Function of proteoglycans in the extracellular matrix. *Acta Patholigica Japonica*, 43(6):283–293, 1993.

Chengxuan Ying, Tianle Cai, Shengjie Luo, Shuxin Zheng, Guolin Ke, Di He, Yanming Shen, and Tie-Yan Liu. Do transformers really perform badly for graph representation? *Advances in neural information processing systems*, 34:28877–28888, 2021.

Zhaoning Yu and Hongyang Gao. Molecular representation learning via heterogeneous motif graph neural networks. In *International Conference on Machine Learning*, pp. 25581–25594. PMLR, 2022.

D Zhang et al. Dnagpt: A generalized pre-trained tool for versatile dna sequence analysis tasks. *Preprint at https://doi. org/10.48550/arXiv*, 2307, 2023a.

Xiao-Lian Zhang. Roles of glycans and glycopeptides in immune system and immune-related diseases. *Current medicinal chemistry*, 13(10):1141–1147, 2006.

Zuobai Zhang, Minghao Xu, Arian Jamasb, Vijil Chenthamarakshan, Aurelie Lozano, Payel Das, and Jian Tang. Protein representation learning by geometric structure pretraining. 2023b.

Zuobai Zhang, Minghao Xu, Aurelie C Lozano, Vijil Chenthamarakshan, Payel Das, and Jian Tang. Pre-training protein encoder via siamese sequence-structure diffusion trajectory prediction. *Advances in Neural Information Processing Systems*, 36, 2024.

Yichong Zhao, Kenta Oono, Hiroki Takizawa, and Masaaki Kotera. Generrna: A generative pre-trained language model for de novo rna design. *bioRxiv*, pp. 2024–02, 2024.

Zhaocheng Zhu, Chence Shi, Zuobai Zhang, Shengchao Liu, Minghao Xu, Xinyu Yuan, Yangtian Zhang, Junkun Chen, Huiyu Cai, Jiarui Lu, et al. Torchdrug: A powerful and flexible machine learning platform for drug discovery. *arXiv preprint arXiv:2202.08320*, 2022.

Wanru Zhuang, Jia Song, Yaqi Li, Shuqi Lu, et al. Pre-training protein bi-level representation through span mask strategy on 3d protein chains. In *International Conference on Machine Learning*. PMLR, 2024.

A APPENDIX

A.1 ACCURACY AND PERPLEXITY CURVES DURING PRE-TRAINING

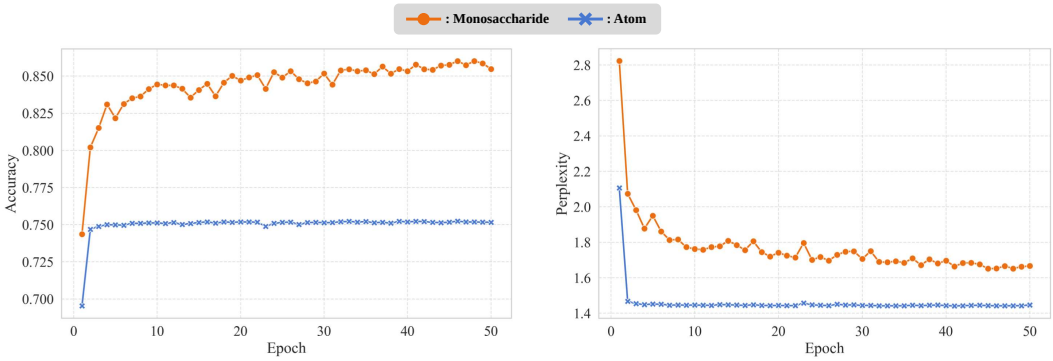

(a) Accuracy over Epochs during Pre-training **(b) Perplexity over Epochs during Pre-training**

Figure 5: The accuracy and perplexity curves during the pre-training phase of PreGlycanAA.

In this appendix, we present the accuracy and perplexity curves that are obtained during the pre-training phase of PreGlycanAA. These curves provide valuable insights into the learning dynamics and the effectiveness of the proposed pre-training method.

Accuracy curve: The accuracy curves in Figure 5(a) illustrate the model's ability to recover masked atoms and monosaccharides correctly along the pre-training process. The initial steep incline suggests rapid learning in the early stage, followed by a gradual approach towards an asymptote, signifying the model's convergence. We can observe the slower convergence of the monosaccharide recovery accuracy compared to the atom recovery accuracy, indicating that the masked monosaccharide prediction task is harder to learn.

Perplexity curve: Perplexity is a measurement of how well a probability distribution predicts a sample, often used in the context of language modeling Devlin (2018). A lower perplexity indicates that the model is more confident at recovering masked elements to their true values. The perplexity curves in Figure 5(b) reflect the reduction of model's uncertainty as pre-training proceeds. Similar to accuracy curves, the convergence of the monosaccharide recovery perplexity is slower than that of the atom recovery perplexity, again indicating the higher difficulty of the masked monosaccharide prediction task.

A.2 ADDITIONAL VISUALIZATION OF GLYCAN REPRESENTATIONS

In Figure 6, we present the glycan representations extracted by GlycanAA and PreGlycanAA on the datasets of eight glycan taxonomy prediction tasks, where GlycanAA is randomly initialized and PreGlycanAA is pre-trained. We employ the t-SNE algorithm (Van der Maaten & Hinton, 2008) for dimensionality reduction.

According to these results, we can observe the better clustering behavior of PreGlycanAA, where it more effectively separates the samples of different classes and gathers the samples of the same class together. This phenomenon is more visually significant on the tasks with fewer classes, *e.g.*, domain and kingdom prediction tasks. The better clustering behavior of PreGlycanAA leads to its superior performance over GlycanAA on 5 out of 8 taxonomy prediction tasks, as shown in Table 1.

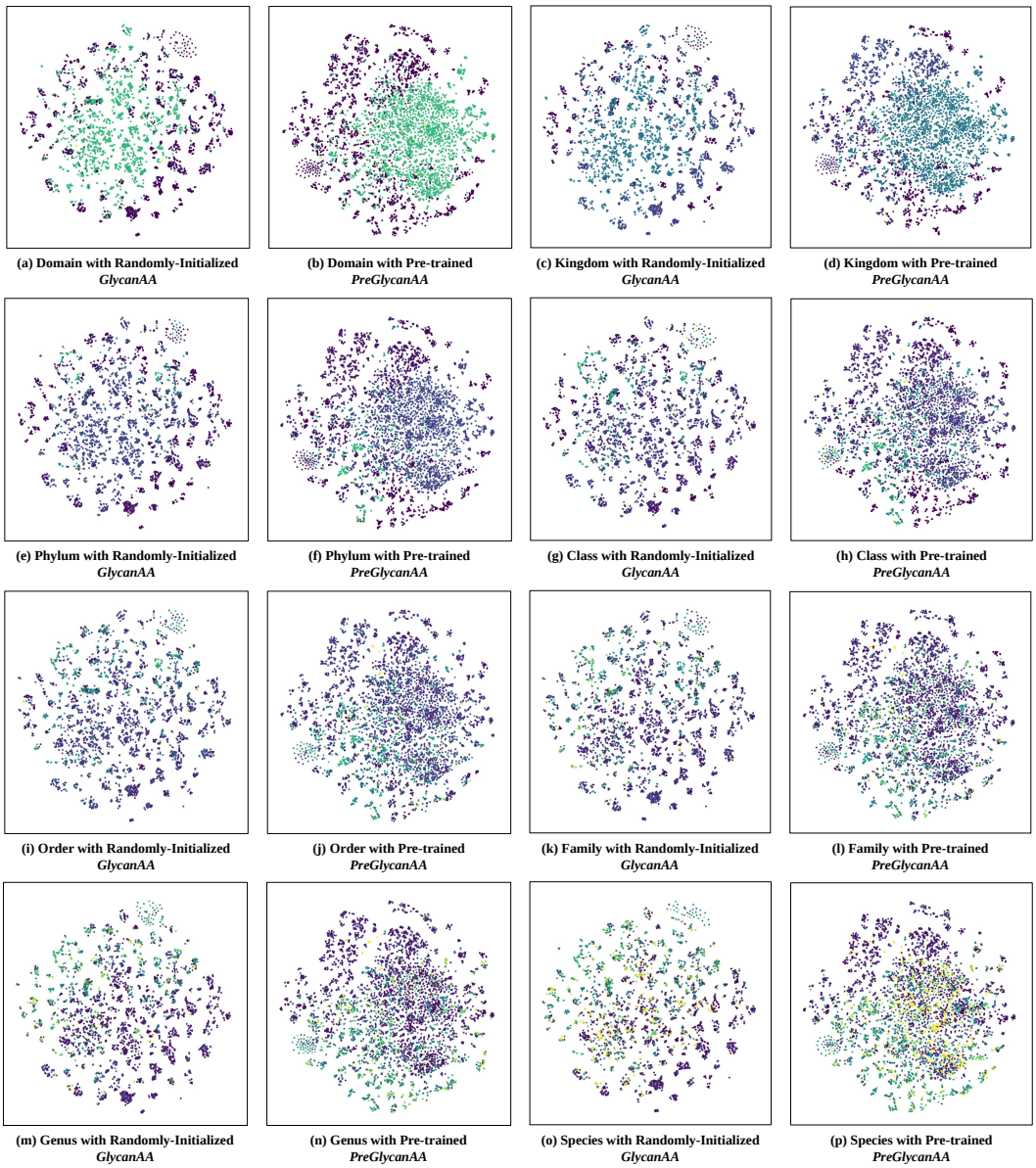

(a) Domain with Randomly-Initialized *GlycanAA*
(b) Domain with Pre-trained *PreGlycanAA*
(c) Kingdom with Randomly-Initialized *GlycanAA*
(d) Kingdom with Pre-trained *PreGlycanAA*
(e) Phylum with Randomly-Initialized *GlycanAA*
(f) Phylum with Pre-trained *PreGlycanAA*
(g) Class with Randomly-Initialized *GlycanAA*
(h) Class with Pre-trained *PreGlycanAA*
(i) Order with Randomly-Initialized *GlycanAA*
(j) Order with Pre-trained *PreGlycanAA*
(k) Family with Randomly-Initialized *GlycanAA*
(l) Family with Pre-trained *PreGlycanAA*
(m) Genus with Randomly-Initialized *GlycanAA*
(n) Genus with Pre-trained *PreGlycanAA*
(o) Species with Randomly-Initialized *GlycanAA*
(p) Species with Pre-trained *PreGlycanAA*

Figure 6: Visualization of glycan representations extracted by GlycanAA and PreGlycanAA on taxonomy prediction tasks. We use different colors to indicate the glycans of different classes, and the color-class correspondence is omitted for concision (many tasks own hundreds of classes).